View metadata, citation and similar papers at core.ac.uk

brought to you by CORE

provided by HKU Scholars Hub

The HKU Scholars Hub The University of Hong Kong 香港大學學術庫

Title	A transverse flux permanent magnet linear generator for hybrid electric vehicles
Author(s)	Li, WL; Lee, CHT; Ching, TW
Citation	The 2013 IEEE International Symposium on Industrial Electronics (ISIE 2013), Taipei, Taiwan, 27-31 May 2013. In Proceedings, 2013, p. 1-6
Issued Date	2013
URL	http://hdl.handle.net/10722/191596
Rights	IEEE International Symposium on Industrial Electronics Proceedings. Copyright © IEEE.

A Transverse Flux Permanent Magnet Linear Generator for Hybrid Electric Vehicles

Wenlong Li, Christopher H. T. Lee
Department of Electrical and Electronic Engineering
The University of Hong Kong
Hong Kong, China
wlli@eee.hku.hk, htlee@eee.hku.hk

T. W. Ching
Faculty of Science and Technology
University of Macau
Macau, China
twching@ieee.org

***Abstract*—This paper presents a transverse flux permanent magnet (TFPM) linear generator for the free-piston generation application, which not only possessing the merits of the existing TFPM machine, but also providing a simple structure which is essential for power generation with maintenance-free operation. Also, the machine configuration is optimized such that the induced voltage is maximized while the cogging force is minimized. Hence, a 2-phase linear TFPM is resulted, which is well supported by performance analysis.**

Keywords— transverse flux;permanent magnet, linear generator; hybrid electric vehicles .

I. INTRODUCTION

With increasing concerns on serious environment pollution and exhausted natural resources, green transportation concept is accepted widely all around the world. Automobiles, which are the key elements in the transportation, need electrification for emission reduction and fuel efficiency improvement. Therefore, the development of electric vehicles (EVs) is in a rapid pace in recent years [1]-[5]. Definitely, the pure EVs, also called as battery EVs, are the best solution to eliminate the vehicle emission problems. However, due to the limit capacity of the battery pack, the wide application is not possible at the current stage. Consequently, the hybrid electric vehicles (HEVs), which use both internal combustion engine (ICE) and electric motor for vehicle operation, dominate the automobile markets. Since the electric motors are involved for vehicle propulsion, on-board electricity generation is indispensible for most of the hybrid electric vehicles. As shown in Fig. 1, the free-piston generator, which consists of a free-piston engine and a linear generator, exhibits a high efficiency and flexibility for electricity production [6]-[8].

In recent years, various rotational permanent magnet (PM) generators have been developed for harnessing renewable energy and electric vehicles, because of their inherently high efficiency and high power density [9]-[10]. Among these rotational PM generators, including the doubly salient PM machine [11]-[25], PM hybrid machine [26]-[29], double-stator PM machine [30]-[31], flux-switching PM machine [32]-[34], flux-mnemonic PM machine [35]-[38] and transverse flux PM (TFPM) machine [39]-[40], the TFPM generator takes the definite merits of higher power density and higher efficiency than the others, as well as the uniqueness that it can be readily transformed from its radial-field morphology into the linear-field morphology. However, it still suffers from a prominent drawback that it usually complies with a complicated structure and hence increases the manufacturing difficulty.

The purpose of this paper is to propose a new TFPM linear generator for free-piston generators, which not only retains the inherent advantages of the existing TFPM machine, but also overcomes the problem of complicated structure. Firstly, the idea will be brought forward by using a 3-phase TFPM generator. Then, it will be extended to derive a new 2-phase TFPM linear generator. Finally, the configuration of this generator will be optimized to maximize the induced electromotive force (EMF) and minimize the cogging force.

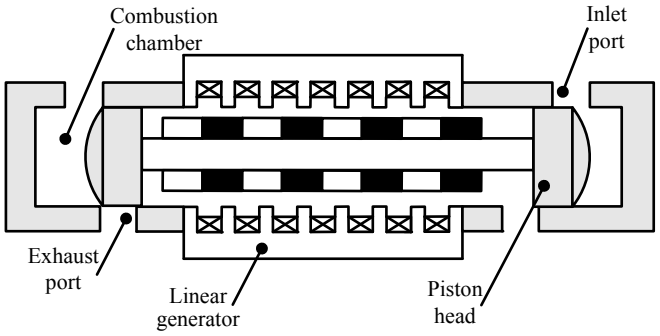

Fig. 1. Free piston engine based generator.

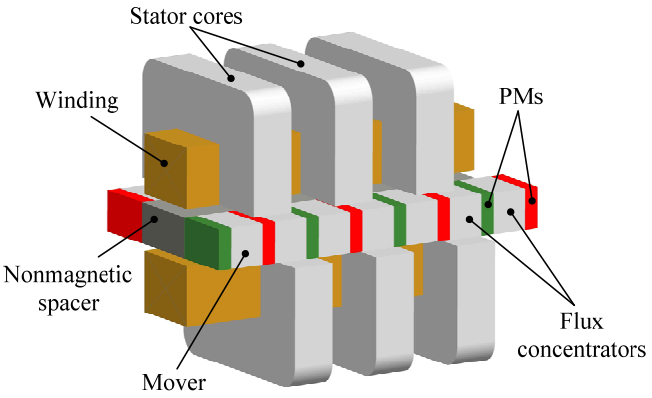

Fig. 2. Configuration of traditional TFPM machine.

II. MACHINE DESIGN

The traditional 3-phase TFPM machine configuration is depicted in Fig. 2. It adopts the double-stator arrangement with the rotor/mover sandwiched between the two stators. Its stator consists of U-shaped cores and windings on both sides of the mover. The U-shaped cores of the upper stator and the lower stator have a separation of a PM pole-pitch to form the flux path. Its mover consists of two rows of PMs and flux concentrators with nonmagnetic material in between. The stator has two sets of windings placed in the upper and lower stator core, respectively. Since their magnetic flux paths via the upper and lower U-shaped stator cores are orthogonal to the current flow of the armature winding, the magnetic loading is totally decoupled from the electric loading. Hence, the corresponding electric loading can be much higher than that of its longitudinal-flux counterpart. The corresponding structure is very complicated such that its reliability and robustness are deteriorated, which are undesirable for the free-piston generator.

In contrast, the proposed 3-phase TFPM linear generator is shown in Fig. 3, which the stator contains three segments of C-shaped iron cores as embraced by armature windings, while the mover consists of 7 PM pole-pairs moving in between the C-shaped iron cores. Because of the inherent decoupling nature in space between the electric circuit and the magnetic circuit, the proposed TFPM linear generator can be designed with a greater number of turns per coil and thus resulting with larger EMF magnitude and higher power density. Fig. 4 depicts the structure of C-shaped iron core. This C-shaped stator structure and the PM segments of the mover are simple and can be easily manufactured, thus solving the problem of complicated structure that usually occurs at conventional TFPM machines. The key design data of the proposed TFPM linear generator are listed in Table I.

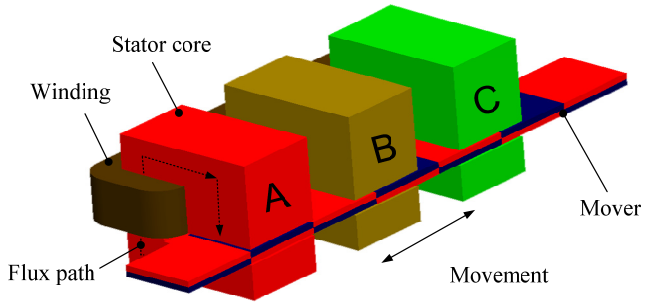

Fig. 3. Proposed 3-phase linear TFPM generator.

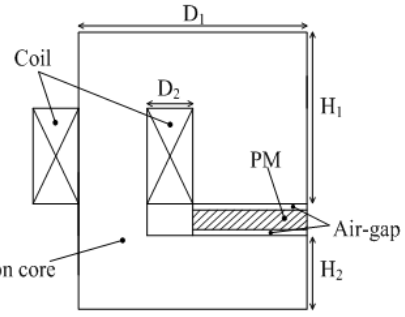

Fig. 4. Structure of C-shaped iron core.

TABLE I. KEY DESIGN DATA

Item	Value
D_1 (mm)	100
D_2 (mm)	20
H_1 (mm)	70
H_2 (mm)	30
Core width (mm)	45
Mover length (mm)	350
Tooth pitch (mm)	83.3
Pole pitch (mm)	50
Air-gap length (mm)	1.5
No. of turns per phase	2100
PM dimension (mm)	10 × 50 × 50
B_r (T)	1.1
H_c (kA/m)	837

III. MACHINE ANALYSIS

The induced EMF of the proposed generator can be expressed as:

$$V = N\frac{d\phi}{dt} = N\,S\frac{dB_c}{dt} \tag{1}$$

where ϕ is the flux in the iron core, S is the cross-sectional area of iron core, and B_c is the flux density in the iron core. The cogging force can be expressed as:

$$W_{co} = \frac{B_a^{\,2}}{2\mu_o}\delta\, x\, l \tag{2}$$

where W_{co} is the magnetic co-energy, x is the displacement in the axial direction, B_a is the flux density in the air-gap, μo is the permeability of free space, δ is air-gap length and l is the length of the mover. Thus, the cogging force can be written as [41]:

$$F = \frac{\partial W_{co}}{\partial x} = \frac{B_a^{\,2}}{2\mu_o}\delta\, l \tag{3}$$

Provided that the flux density distribution is known, the induced EMF and cogging force can be determined by using (1) and (3), respectively. Although the magnetic circuits of the proposed generator is 3D in nature, the use of 3D finite element method (FEM) to perform analysis and optimization is too tedious and actually unnecessary [7]. Since the yoke of each stator of the proposed generator is equivalent to the tooth with a periodic boundary, the 2D FEM can be employed for analysis. Hence, the magnetic field distribution can be easily obtained as shown in Fig. 5. Then, the corresponding air-gap flux density waveform is deduced as shown in Fig. 6 in which the peak value can reach to 1.2 T, which confirm its merit of high power density. When the mover speed is set to be 1 m/s, the induced EMF can be simulated with the peak-to-peak value of phase-A equal to 315 V as depicted in Fig. 7. Also, the cogging force and normal force are simulated as depicted in Fig. 8 and Fig. 9.

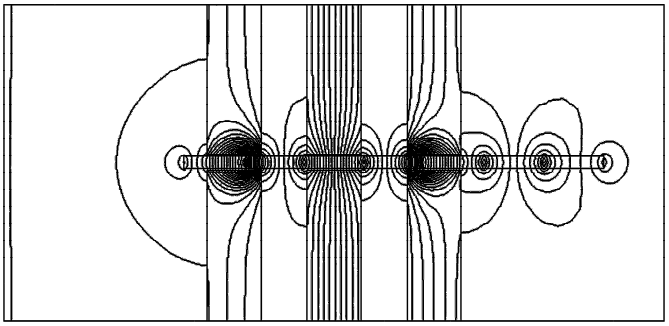

Fig. 5. Magnetic field distribution of proposed 3-phase generator.

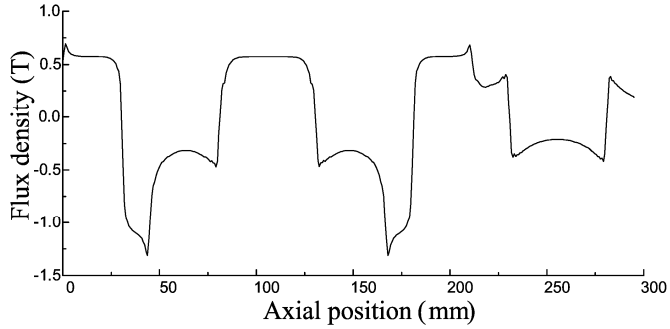

Fig. 6. Air-gap flux density waveform of proposed 3-phase generator.

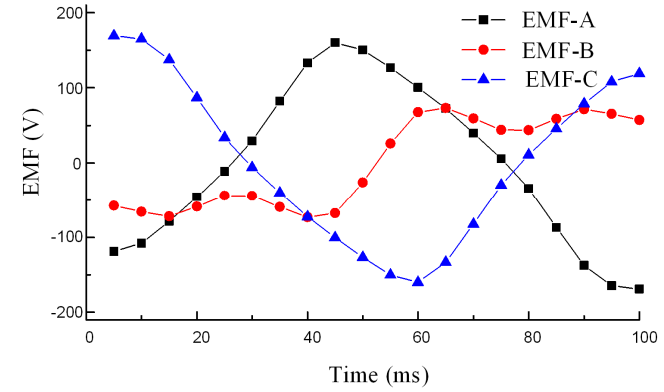

Fig. 7. EMF waveform of proposed 3-phase generator.

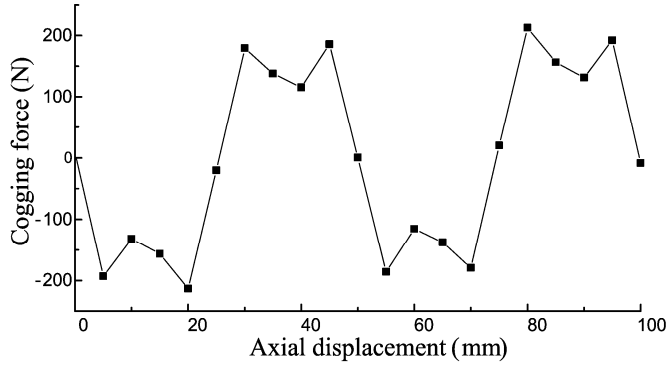

Fig. 8. Cogging force waveform of proposed 3-phase generator.

IV. Machine Optimization

The shortcomings of the mentioned 3-phase configuration are obvious: namely, the phase differences are not equal; the phase-B is highly distorted; the cogging force is too large. The major reason is due to the fact that the reluctance of the magnetic flux path via the middle iron core is greatly influenced by the adjacent iron cores. In order to solve this problem, the fourth C-shaped iron core is added while the mover is lengthened to 9 PM pole-pairs. Meanwhile, the first and the third armature windings are series-opposing connected together to form a new phase-A, while the second and the fourth armature windings are also series-opposing connected together to form a new phase-B. Thus, the adverse effect on the reluctance of the middle iron core due to the adjacent iron cores can be compensated from one another. The resulting 2-phase TFPM linear generator is shown in Fig. 10.

Based on the same key data as the 3-phase counterpart, the induced EMF waveform and the cogging force waveform of this 2-phase TFPM linear generator are simulated as shown in Fig. 11 and Fig. 12, respectively. It can be observed that the peak-to-peak value of induced EMF is 588 V which is much larger than the 315V produced by the 3-phase one. Also, the cogging force is greatly suppressed, namely about a half of the 3-phase one.

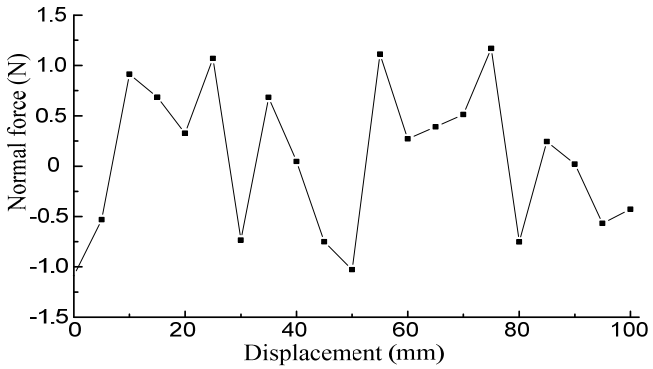

Fig. 9. Normal force waveform of proposed 3-phase generator.

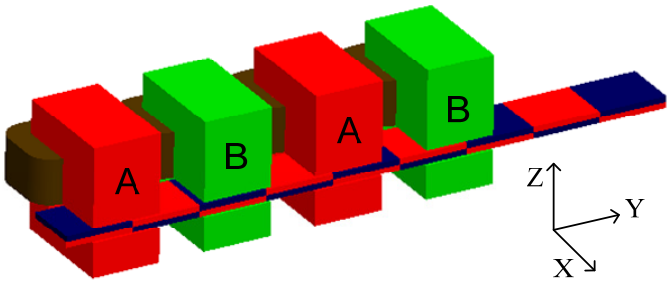

Fig. 10. Proposed 2-phase linear TFPM generator.

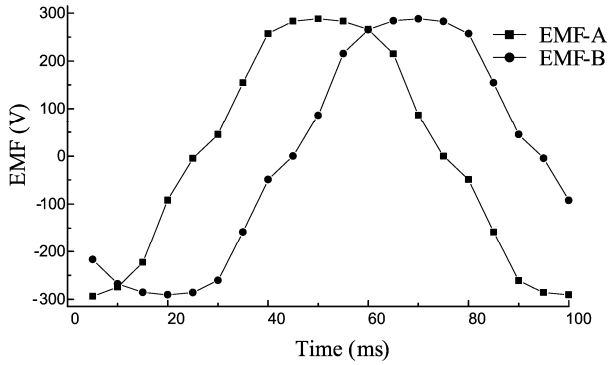

Fig. 11. EMF waveform of proposed 2-phase generator.

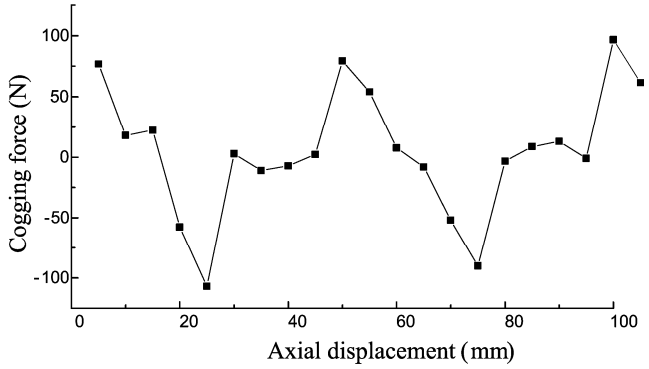

Fig. 12. Cogging force waveform of proposed 2-phase generator.

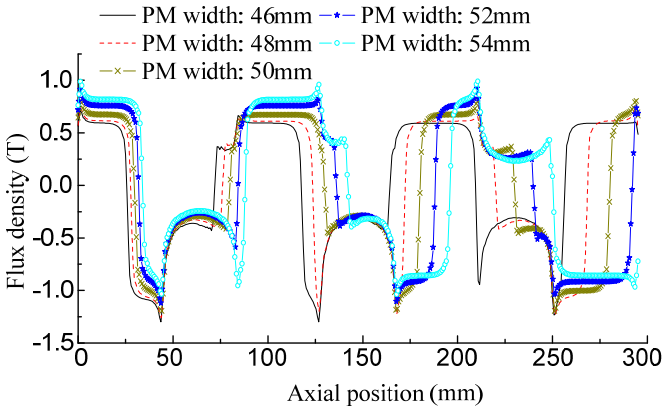

Fig. 13. Air-gap flux density waveforms of proposed 2-phase generator.

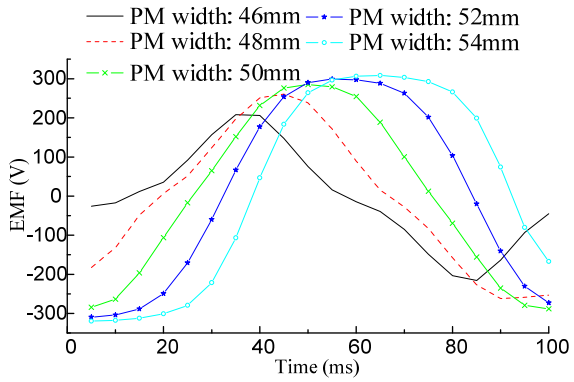

Fig. 14. EMF waveforms of proposed 2-phase generator.

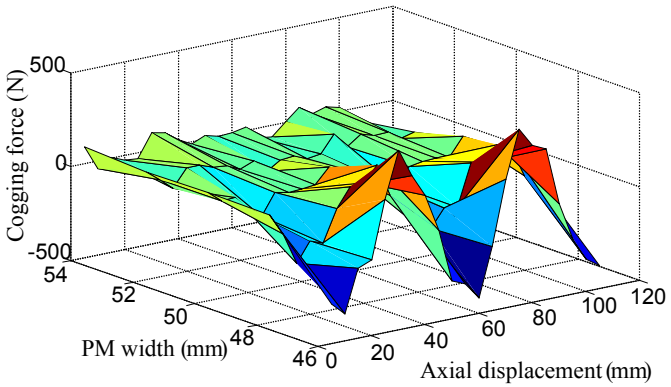

Fig. 15. Cogging force characteristics of proposed 2-phase generator.

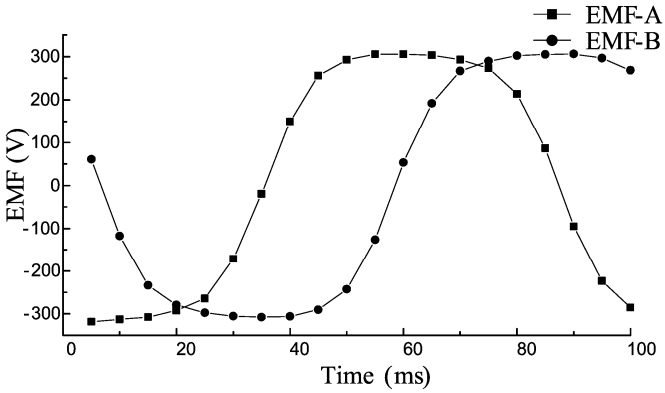

Fig. 16. Optimized EMF waveforms of proposed 2-phase generator.

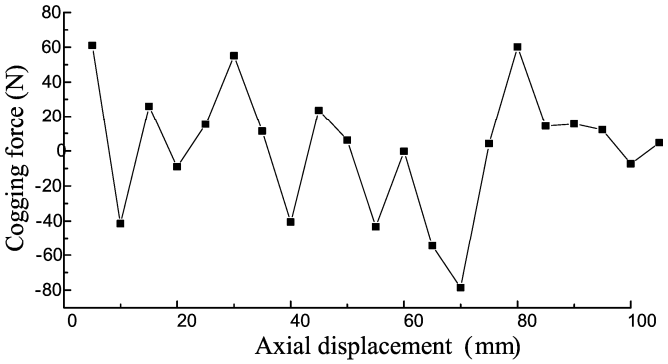

Fig. 17. Optimized cogging waveform of proposed 2-phase generator.

There are two important indicators of this linear generator: The first one is the amplitude and shape of the induced EMF waveforms which reflect the power quality of electricity generation; the second one is the value of cogging torque waveform which reflects the usefulness of smooth free-piston generator operation. So, the optimization of the proposed 2-phase generator focuses on maximizing the amplitude and symmetry of the induced EMF and on minimizing the cogging force. Since both indicators are mainly affected by the flux density, the PM width and the core width are selected as the variable parameters for optimization.

Firstly, the PM width varies from 46 mm (92% of nominal) to 54 mm (108% of nominal) while the core width is kept unchanged. The corresponding air-gap flux density waveforms are depicted in Fig. 13. Hence, the EMF waveforms are

obtained as shown in Fig. 14. It can be found that both the amplitude and symmetry generally increase with the PM width. The width of 52 mm is considered to be optimal since an additional increase of the PM width does not offer significant additional improvement. On the other hand, the cogging force characteristics are depicted in Fig. 15. It illustrates that the corresponding peak value decreases from 440 N to 70 N when the PM width increases from 46 mm to 52 mm. This phenomenon can be reflected from Fig. 13 that the peak value of air-gap flux densities decreases gradually as the PM width increases from 46 mm to 52 mm.

Secondly, the core width is varied while the PM width is kept constant at 52 mm. It can be deduced that the optimal core width is 43 mm. So, when picking up these two optimal parameters, the optimized EMF waveforms of the proposed 2-phase generator are depicted in Fig. 16. It can be observed that these waveforms are very symmetric in trapezoidal form and have a phase difference of approximately 90°. The corresponding peak-to-peak value can achieve 630 V, which is better than the non-optimized one (588 V) and much greater than the 3-phase counterpart (315 V). These EMF waveforms are highly attractive for on-board power generation, since their rectified version can readily be converted for battery charging. Finally, the optimized cogging force is shown in Fig. 17. The corresponding peak value is only 35% of its 3-phase counterpart.

V. CONCLUSION

In this paper, a new 2-phase TFPM linear generator has been proposed and optimized for free-piston generators. This generator not only retains the merits of the existing TFPM machine, but also offers a unique simple structure that can be easily fabricated and assembled. By fine tuning the PM width and core width of the proposed generator, the optimized EMF can reach to a high voltage amplitude while exhibit a symmetric and trapezoidal waveform which is highly desirable for power processing. Also, the optimized cogging force is low enough to effectively operate in the free-piston generator.

ACKNOWLEDGMENT

This work was supported by a grant (Project No. HKU710711E) from the Hong Kong Research Grants Council, Hong Kong Special Administrative Region, China.

REFERENCES

[1] C.C. Chan and K.T. Chau, Modern Electric Vehicle Technology. Oxford: Oxford University Press, 2001.

[2] K.T. Chau and C.C. Chan, "Emerging energy-efficient technologies for hybrid electric vehicles," Proceedings of IEEE, vol. 95, no. 4, April 2007, pp. 821-835.

[3] K.T. Chau, Electric Motor Drives for Battery, Hybrid and Fuel Cell Vehicles. In Electric Vehicles: Technology, Research and Development, ed. G.B. Raines. Nova Science Publishers, December 2009, pp. 1-40.

[4] M. Ehsani, Y. Gao and A. Emadi, Modern Electric, Hybrid Electric, and Fuel Cell Vehicles: Fudamental, Theory, and Design. Taylor and Francis Group, 2009.

[5] K.T. Chau, Hybrid Vehicles. In Alternative Fuels for Transportation, ed. A.S. Ramadhas. CRC Press / Taylors and Francis Group, November 2010, pp. 361-391.

[6] R. Mikalsen and A. P. Roskilly, A review of free-piston engine history and applications, Applied Thermal Engineering, Vol. 27, No. 14-15, 2339-2352, 2007.

[7] W. Li and K.T. Chau, "A linear magnetic-geared free-piston generator for range-extended electric vehicles," Journal of Asian Electric vehicles, vol. 8, no.1, 2010, pp. 1345-1349.

[8] J. Lim, S. Hong and H. Jung, "Design and analysis of 5 kw class tubular type linear generator for free-piston engine," vol. 35, no. 4, International Journal of Applied Eletromagnetics and Mechanics, 2011, pp. 231-240.

[9] K.T. Chau, W. Li and C.H.T. Lee, "Challenges and opportunities of electric machines for renewable energy," Progress In Electromagnetics Research B, vol. 42, 2012, pp. 45-74.

[10] K. T. Chau and W. Li, "Overview of electric machines for electric and hybrid vehicles," International Journal of Vehicle Design, In press.

[11] Z.Q. Zhu, Y. Pang, W. Hua, M. Cheng, and D. Howe, "Investigation of end-effect in PM brushless machines having magnets in the stator," Journal of Applied Physics, vol. 99, no. 8, April 2006, pp.08R319:1-3.

[12] K.T. Chau, M. Cheng, and C.C. Chan, "Performance analysis of 8/6-pole doubly salient permanent magnet motor," Electric Machines and Power Systems, vol. 27, no. 10, October 1999, pp. 1055-1067.

[13] M. Cheng, K.T. Chau, C.C. Chan, E. Zhou and X. Huang, "Nonlinear varying-network magnetic circuit analysis for doubly salient permanent magnet motors," IEEE Transactions on Magnetics, vol. 36, no. 1, January 2000, pp. 339-348.

[14] M. Cheng, K.T. Chau, C.C. Chan, and E. Zhou, "Performance analysis of split-winding doubly salient permanent magnet motor for wide speed operation," Electric Machines and Power Systems, vol. 28, no. 3, March 2000, pp. 277-288.

[15] Y. Liao, F. Liang and T.A. Lipo, "A novel permanent magnet motor with doubly salient structure," IEEE Transactions on Industry Applications, vol. 31, no. 5, Sep/Oct 1995, pp. 1069-1078.

[16] M. Cheng, K.T. Chau, and C.C. Chan, "Design and analysis of a new doubly salient permanent magnet motor," IEEE Transactions on Magnetics, vol. 37, no. 4, July 2001, pp. 3012-3020.

[17] K.T. Chau, M. Cheng and C.C. Chan, "Nonlinear magnetic circuit analysis for a novel stator-doubly-fed doubly-salient machine," IEEE Transactions on Magnetics, vol. 38, no. 5, September 2002, pp. 2382-2384.

[18] Y. Li and C.C. Mi, "Doubly salient permanent-magnet machine with skewed rotor and six-state commutating mode," IEEE Transactions on Magnetics, vol. 43, no. 9, September, 2007, pp. 3623-3629.

[19] M. Cheng, K.T. Chau and C.C. Chan, "New split-winding doubly salient permanent magnet motor drive," IEEE Transactions on Aerospace and Electronic Systems, vol. 39, no. 1, January 2003, pp. 202-210.

[20] K.T. Chau, Q. Sun, Y. Fan and M. Cheng, "Torque ripple minimization of doubly salient permanent magnet motors," IEEE Transactions on Energy Conversion, vol. 20, no. 2, June 2005, pp. 352-358.

[21] R.P. Deodhar, S. Andersson, I. Boldea and T.J.E. Miller, "The flux-reversal machine: a new brushless doubly-salient permanent-magnet machine," IEEE Transactions on Industry Applications, vol. 33, no. 4, Jul/Aug 1997, pp. 925-934.

[22] Y. Fan, K.T. Chau and M. Cheng, "A new three-phase doubly salient permanent magnet machine for wind power generation," IEEE Transactions on Industry Applications, vol. 42, no. 1, January/February 2006, pp. 53-60.

[23] K.T. Chau, Y.B. Li, J.Z. Jiang and C. Liu, "Design and analysis of a stator-doubly-fed doubly-salient permanent-magnet machine for automotive engines," IEEE Transactions on Magnetics, vol. 42, no. 10, October 2006, pp. 3470-3472.

[24] Y. Gong, K.T. Chau, J.Z. Jiang, C. Yu and W. Li, "Analysis of doubly salient memory motors using Preisach theory," IEEE Transactions on Magnetics, vol. 45, no. 10, October 2009, pp. 4676-4679.

[25] W. Zhao, K.T. Chau, M. Cheng, J. Ji and X. Zhu, "Remedial brushless AC operation of fault-tolerant doubly-salient permanent-magnet motor

drives," IEEE Transactions on Industrial Electronics, vol. 57, no. 6, June 2010, pp. 2134-2141.

[26] C. Liu, K.T. Chau, J.Z. Jiang and L. Jian, "Design of a new outer-rotor permanent magnet hybrid machine for wind power generation," IEEE Transactions on Magnetics, vol. 44, no. 6, June 2008, pp. 1494-1497.

[27] Z. Zhang, Y. Tao and Y. Yan, "Investigation of a new topology of hybrid excitation doubly salient brushless DC generator," IEEE Transactions on Industrial Electronics, vol. 59, no. 6, June 2012, pp. 2550-2556.

[28] C. Liu, K.T. Chau and X. Zhang, "An efficient wind-photovoltaic hybrid generation system using doubly-excited permanent-magnet brushless machine," IEEE Transactions on Industrial Electronics, vol. 57, no. 3, March 2010, pp. 831-839.

[29] C. Liu, K.T. Chau and W. Li, "Comparison of fault-tolerant operations for permanent-magnet hybrid brushless motor drive," IEEE Transactions on Magnetics, vol. 45, no. 6, June 2010, pp. 1378-1381.

[30] S. Niu, K.T. Chau, J.Z. Jiang and C. Liu, "Design and control of a new double-stator cup-rotor permanent-magnet machine for wind power generation," IEEE Transactions on Magnetics, vol. 43, no. 6, June 2007, pp. 2501-2503.

[31] S. Niu, K.T. Chau and C. Yu, "Quantitative comparison of double-stator and traditional permanent magnet brushless machines," Journal of Applied Physics, vol. 105, no. 7, April 2009, paper no. 07F105, pp. 1-3.

[32] J.T. Chen and Z.Q. Zhu, "Winding configurations and optimal stator ans rotor pole combination of flux-switching PM brushless AC machines," IEEE Transactions on Energy Conversion, vol. 25, no. 2, June 2010, pp.293-302.

[33] H. Jia, M. Cheng, W. Hua, W.X. Zhao and W. Li, "Torque ripple suppression in flux-switching PM motor by harmonic current injection based on voltage space-vector modulation," IEEE Transactions on Magnetics, vol. 46, no. 6, June 2010, pp.1527-1530.

[34] W. Hua, M. Cheng, Z. Q. Zhu and D. Howe, "Analysis and optimization of back-emf waveform of a novel flux-switching permanent magnet motor," IEEE Transactions on Energy Conversion, vol. 23, no. 3, September 2008, pp.727-733.

[35] C. Yu, K.T. Chau, X. Liu and J.Z. Jiang, "A flux-mnemonic permanent magnet brushless motor for electric vehicles," Journal of Applied Physics, vol. 103, no. 7, April 2008, paper no. 07F103, pp. 1-3.

[36] X. Zhu, K.T. Chau, M. Cheng and C. Yu, "Design and control of a flux-controllable stator-permanent magnet brushless motor drive," Journal of Applied Physics, vol. 103, no. 7, April 2008, paper no. 7F134, pp. 1-3.

[37] J.H. Lee and J.P. Hong, "Permanent magnet demagnetization characteristic analysis of a variable flux memory motor using coupled preisach modeling and FEM," IEEE Transactions on Magnetics, vol. 44, no. 6, June 2008, pp. 1550-1553.

[38] X. Zhu, L. Quan, D. Chen, M. Cheng, Z. Wang and W. Li, "Design and analysis of a new flux memory doubly salient motor capable of online flux control. IEEE Transactions on Magnetics, vol. 47, no. 10, October 2011, pp.3220-3223.

[39] J. Wang, K.T. Chau, J.Z. Jiang and C. Yu, "Design and analysis of a transverse flux permanent magnet machine using three dimensional scalar magnetic potential finite element method," Journal of Applied Physics, vol. 103, no. 7, April 2008, pp. 7F107:1-3.

[40] W. Li and K.T. Chau, "Design and analysis of a novel linear transverse flux permanent magnet motor using HTS magnetic shielding," IEEE Transactions on Applied Superconductivity, vol. 20, no. 3, June 2010, pp. 1106-1109.

[41] D.H. Kang, Y.H. Jeong and M.H. Kim, "A study on the design of transverse flux linear motor with high power density," Proceeding of International Symposium on Industrial Electronics, vol. 2, Pusan, Korea, 2001, pp. 707-711.